Published in final edited form as:

Circ Cardiovasc Imaging. 2017 June ; 10(6): . doi:10.1161/CIRCIMAGING.116.003951.

Recent Advances in Cardiovascular Magnetic Resonance Techniques and Applications

Michael Salerno, MD, PhD, **Behzad Sharif, PhD**, **Håkan Arheden, MD, PhD**, **Andreas Kumar, MD, MSc**, **Leon Axel, MD, PhD**, **Debiao Li, PhD**, and **Stefan Neubauer, MD**

Cardiovascular Division, Department of Medicine, Department of Radiology and Medical Imaging, and Department of Biomedical Engineering, University of Virginia Health System, Charlottesville (M.S.); Biomedical Imaging Research Institute, Department of Biomedical Sciences, Cedars-Sinai Medical Center, Los Angeles, CA (B.S., D.L.); Department of Clinical Sciences, Clinical Physiology, Lund University, Skane University Hospital, Sweden (H.A.); Cardiology Division, Department of Medicine, Northern Ontario School of Medicine, Sudbury, Canada (A.K.); Department of Radiology and Department of Medicine, New York University, New York (L.A.); and Division of Cardiovascular Medicine, Oxford Center for Clinical Magnetic Resonance Research, University of Oxford, London, United Kingdom (S.N.)

Abstract

Cardiovascular magnetic resonance imaging has become the gold standard for evaluating myocardial function, volumes, and scarring. Additionally, cardiovascular magnetic resonance imaging is unique in its comprehensive tissue characterization, including assessment of myocardial edema, myocardial siderosis, myocardial perfusion, and diffuse myocardial fibrosis. Cardiovascular magnetic resonance imaging has become an indispensable tool in the evaluation of congenital heart disease, heart failure, cardiac masses, pericardial disease, and coronary artery disease. This review will highlight some recent novel cardiovascular magnetic resonance imaging techniques, concepts, and applications.

Keywords

compressed sensing; extracellular volume; magnetic resonance imaging; myocardial perfusion; navigator gating; T1 mapping

---

Cardiovascular magnetic resonance (CMR) is now a mature imaging modality and has become the gold standard technique for evaluating myocardial function, quantifying myocardial volumes, and detecting myocardial scar. CMR has the unique ability to provide detailed tissue characterization, including assessment of edema, iron overload, and diffuse myocardial fibrosis. Recent guidelines and appropriate use criteria documents increasingly

---

Correspondence to Michael Salerno, MD, PhD, Associate Professor of Medicine, Radiology, and Biomedical Engineering, University of Virginia Health System, 1215 Lee St, Box 800158, Charlottesville, VA 22908. ms5pc@virginia.edu.

Disclosures

Dr Sharif receives research support from Astellas Pharma US, Inc. Dr Salerno receives research support from Astra Zeneca. Dr Arheden is a shareholder of Imacor AB, Lund, Sweden. Dr Neubauer acknowledges support from the Oxford NIHR Biomedical Research Centre and from the Oxford British Heart Foundation Centre of Research Excellence. The other authors report no conflicts.

include new indications for CMR for the evaluation of congenital heart disease, heart failure, and coronary artery disease (CAD). CMR is a field characterized by ongoing technical development producing many novel clinical applications, and as such, this review will describe only a subset of evolving CMR techniques.

Advanced Image Reconstruction Techniques

Recent advances in image reconstruction techniques have the potential to further increase the clinical utility of CMR by significantly accelerating image acquisition, enabling robust 3-dimensional (3D) volumetric imaging and fostering the development of novel CMR imaging techniques.

Conventional CMR Reconstruction Techniques

Currently, most clinical CMR imaging is performed by sequentially acquiring lines of raw data on a Cartesian grid. This process is inherently slow, and without any acceleration techniques, it would take ≈250 ms to acquire a single image. A single-shot image with this temporal footprint would be corrupted by cardiac motion, and a cine acquisition would have only 4 frames per second. To overcome this limitation and increase effective temporal resolution, most CMR images are acquired in a segmented fashion, where a portion of the total required lines are acquired in each heartbeat during a breath hold, and the acquisition is synchronized to the ECG using cardiac gating. However, because images are synthesized from data acquired over multiple heartbeats, this technique is sensitive to changes in the cardiac cycle length, which occur during arrhythmias, and to changes in respiratory position because of inadequate breath holding. The situation becomes even more challenging for high-resolution, dynamic, or 3D acquisitions, which require even more data to be acquired. Thus, approaches for speeding up CMR image acquisition rely on using other prior information to produce images with fewer lines of data.

Parallel Imaging and k-t-Accelerated Imaging

The number of lines required to accurately reconstruct an image can be reduced using parallel imaging techniques which use differences in the spatial sensitivity of multiple receiver coils placed around the patient to provide the additional information needed for image reconstruction. Parallel imaging approaches are widely used on commercial magnetic resonance imaging systems with acronyms such as Sensitivity Encoding (SENSE), Generalized Autocalibrating Partial Parallel Acquisition (GRAPPA), and Autocalibrating Reconstruction for Cartesian imaging (ARC), but are typically limited to 2- to 3-fold acceleration factors because of the geometry of the coil elements and reduction in signal-to-noise ratio because of acquiring less data.

The amount of data needed for image reconstruction can be further reduced by taking advantage of the correlation between images at different times in the cardiac cycle or between different heartbeats in a dynamic acquisition. Images can be reconstructed with a reduced number of data lines using techniques such as k-t Broad-use Linear Acquisition Speed-up Technique (BLAST),[1] k-t SENSE, or k-t Principal Component Analysis (PCA).[2] These innovative techniques have enabled 3D perfusion imaging, 4-dimensional flow, and

real-time imaging with high temporal and spatial resolution. Accelerations of 12× have been achieved using these techniques for 3D data acquisition.[3] However, these techniques can be corrupted by respiratory motion.

Constrained Reconstruction and Compressed Sensing

An active area of image reconstruction research involves compressed sensing (CS), which enables reconstruction of images from significantly fewer lines of data by relying on the concept that the information content of CMR images is compressible, which is referred to as sparsity. CS has been used for several applications, including perfusion imaging,[4–6] flow imaging,[7] angiography, T1 mapping,[8] and real-time free-breathing cine imaging.[9] The CS technique has also been applied to continuously acquired free-breathing radial techniques, such as in the Extra-Dimensional Golden-angle Radial Sparse Parallel Imaging (XD-GRASP)[10] technique, which enables separation of the data in both cardiac and respiratory dimensions without the need for cardiac gating or breath holding (Figure 1) While these nonstandard reconstruction methods are often computationally demanding, the recent availability of improved computer hardware, such as graphical processing units, is making them practical. CS techniques are still in evolution and will need more research to determine whether they will be robust enough for routine clinical application.

Advanced Techniques and Applications for First-Pass Perfusion CMR

With recent hardware and software improvements, first-pass perfusion imaging using CMR has emerged as an attractive alternative to single photon emission computed tomography myocardial perfusion imaging (MPI) for assessment of patients with suspected CAD. Perfusion is assessed using CMR by imaging the first pass of a gadolinium-based contrast agent (GBCA) through the myocardium during vasodilator stress. Regions that are hypoperfused have a slower uptake and lower concentration of the GBCA and appear as hypointense perfusion defects on the image series.

Current clinically available techniques typically image 3 short-axis myocardial slices (thickness, 8–10 mm) with an in-plane resolution of 2 to 3 mm for conventional methods and <2 mm for advanced high-resolution approaches typically using parallel imaging techniques or k-t acceleration, as described earlier. The diagnostic performance of qualitative perfusion CMR versus single photon emission computed tomography MPI has been studied in multiple clinical trials for detection of significant CAD. The CE-MARC[11] study (Clinical Evaluation of Magnetic Resonance Imaging in Coronary Heart Disease) demonstrated a superior diagnostic performance for perfusion CMR compared with single photon emission computed tomography MPI in 752 patients (area under the receiver-operating characteristic curve, 0.89 versus 0.74; $P<0.001$). The performance of high-resolution perfusion CMR was compared with positron emission tomography MPI in a limited study of 41 CAD patients and demonstrated similar performance both in terms of visual analysis and in terms of quantification of perfusion reserve.[12]

Recent Technical Advances

Whole-Heart Spatial Coverage—Among the most significant recent advancements is the ability to achieve improved spatial coverage, either by extending the number of 2-dimensional slices or by acquiring 3D volumetric data (Figure 2).[3] Unlike nuclear MPI methods, which intrinsically achieve whole-heart coverage, extending the spatial coverage of CMR-based perfusion methods to image the whole heart involves technical trade-offs, such as reducing spatial resolution or increasing the temporal acquisition window, both of which could lead to lower image quality when compared with high-resolution 3-slice methods.[13] However, a recent multicenter study[14] showed excellent diagnostic performance for 3D whole-heart perfusion CMR for detection of functionally significant CAD defined by fractional flow reserve (sensitivity and specificity, 84.7% and 90.8%, respectively).

Improved Imaging of Subendocardial Perfusion—In contrast to nuclear MPI, including positron emission tomography, CMR perfusion imaging has the unique ability to resolve the differences in myocardial perfusion between subepicardial and subendocardial layers because of its potential for high spatial resolution ranging from 1.2 to 3 mm. This is relevant because the subendocardium is the most susceptible layer to ischemia and typically the earliest affected. Conventional CMR techniques, however, are limited by the so-called subendocardial dark-rim artifact (DRA) and may fall short of reliable imaging of subendocardial perfusion.[15] High-resolution (1.4 mm in-plane) perfusion CMR with Cartesian sampling, based on k-t BLAST, reduces the extent of DRA and, thereby, enables accurate detection of subendocardial ischemia, clearly visualizing subendocardial perfusion defects in this patient with 2-vessel CAD (Figure 3A).[16] A different approach involves data acquisition along non-Cartesian patterns, such as spiral and radial trajectories. These techniques are less susceptible to DRA because of their reduced motion sensitivity.[15] Spiral perfusion CMR is effective in reducing DRA,[17,18] enabling visualization of subendocardial perfusion defects (Figure 3B) with good clinical performance in a single-center study.[19] Recent spiral approaches using compressed sensing have enabled wholeheart data acquisition.[6]

Radial imaging has also been shown to be effective in minimizing the DRA.[20] Radial perfusion CMR is well suited for continuous acquisition and self-gating, effectively eliminating the need for ECG gating, and has the potential to achieve high diagnostic accuracy in arrhythmic patients.[21] Radial perfusion imaging, using a slice-interleaved continuous approach (Figure 3C), has demonstrated potential for acquiring high-resolution perfusion images (1.4 mm in-plane) at the end-systolic phase without the need for ECG gating.[5] These techniques are largely experimental and have not been fully validated clinically.

Quantitative Perfusion CMR in CAD and Microvascular Dysfunction—Quantitative perfusion CMR methods have continued to advance, and recent studies have demonstrated incremental diagnostic utility of quantifying absolute myocardial blood flow over visual interpretation and semiquantitative analysis.[22,23] The main challenges for CMR perfusion quantification include a lack of standardization of postprocessing approaches and the overall perception that quantitative perfusion CMR protocols are complex and require

labor-intensive postprocessing. Regarding the latter, several efforts are underway to simplify the data acquisition protocol, for example, eliminating the need for breath holding or ECG gating and to simplify the quantification procedure by enabling fully automatic postprocessing. One of the emerging application areas for perfusion CMR is assessment of coronary microvascular dysfunction, which is typically characterized by signs and symptoms of ischemia in the absence of obstructive CAD. Performance of semiquantitative perfusion CMR for detection of coronary microvascular dysfunction was evaluated in a recent study of 118 women who also underwent coronary reactivity testing, resulting in a sensitivity and specificity of 73% and 74%, respectively.[24] It is expected that quantification of myocardial blood flow and perfusion reserve will further improve the diagnostic performance compared with semiquantitative analysis. Further standardization of techniques and improved inline automatic postprocessing for rapid quantification of myocardial blood flow will be necessary for widespread utility and clinical impact.

Noncontrast Parametric Mapping Techniques

Given recent safety concerns of using GBCAs in patients with impaired renal function, there has been renewed interest in the development of techniques which can perform tissue characterization without the need for contrast agents. These techniques rely on the intrinsic magnetic T1, T2, and T2* relaxation properties of the myocardium. By measuring images with different sensitivity to these intrinsic properties, parametric maps can be created.[25]

T1 Mapping

Native T1 mapping is acquired before the administration of exogenous agents to provide a quantitative map of T1 relaxation times of the tissues being imaged on a pixel-by-pixel basis. Native T1 values reflect signals originating from the intracellular and extracellular (including interstitial and intravascular) compartments and reflect intrinsic differences in tissue properties. A range of T1 mapping techniques are available based on inversion recovery (eg, Modified Look-Locker Imaging [MOLLI],[26] shortened MOLLI [ShMOLLI][27]), saturation recovery (Saturation Recovery Single-Shot Acquisition [SASHA],[28] Saturation Method Using Adaptive Recovery Times for Cardiac T1 Mapping [SMARTT1]), or hybrid techniques (SaturationPulse Prepared Heart Rate Independent Inversion-Recovery [SAPPHIRE]).[29]

Increased native T1 is useful for detecting acute myocardial pathologies, such as edema, infarction, and myocarditis,[30] and subacute cardiomyopathies, such as cardiac amyloidosis, hypertrophic cardiomyopathy, and dilated cardiomyopathy, and for assessing diffuse fibrosis.[29,31–34] Low global myocardial T1 values have clinical utility in myocardial iron overload (siderosis)[35] and Fabry disease.[36] In Anderson–Fabry disease, which is characterized by intramyocardial lipid deposition, low native T1 facilitates differentiation from other causes of left ventricular hypertrophy, such as hypertrophic cardiomyopathy and amyloidosis, which increase native T1. Native T1 mapping can detect the increase in myocardial blood volume associated with coronary vasodilation downstream of significant coronary stenoses.[37] This may potentially be an emerging application to detect myocardial ischemia without the need for GBCA. In addition to its ability to diagnose disease, there is increasing

evidence that native T1 mapping carries prognostic power in risk stratification, including in patients with acute myocardial infarction, amyloidosis, and dilated cardiomyopathy.[29]

T2 Mapping

Myocardial edema plays a role in many disease processes that affect the myocardium, including myocarditis and myocardial infarction. Prior to the widespread availability of T2 mapping pulse sequences, edema was typically imaged using dark-blood T2-weighted spin echo pulse sequences, but these sequences have several inherent limitations. Newly developed T2-mapping sequences can overcome these limitations by quantifying T2 relaxation times.[38] Studies in myocarditis and acute myocardial infarction have consistently demonstrated that T2 mapping provides increased diagnostic accuracy as compared with T2-weighted techniques for detection of myocardial edema.[39,40] T2-mapping techniques are replacing T2-weighted techniques for most diagnostic applications.

New Applications of T2* Mapping

T2* mapping has become well established for the detection of myocardial iron overload and predicts both the progression to heart failure and the requirement for future chelation therapy.[41] However, there are several other important and emerging applications of T2* mapping.

T2* Mapping of Myocardial Infarction—In the early 1980s, myocardial hemorrhage was observed in animal studies as a potential complication of myocardial ischemia and reperfusion injury.[42] Recent studies using T2* mapping have demonstrated that hemorrhagic infarction leads to chronic iron deposition in the myocardial scar, which is associated with ongoing inflammation and monocyte infiltration, specifically colocalized in the iron-deposition zones.[43] In patients with chronic ischemic cardiomyopathy who subsequently received an ICD, early evidence suggests that iron may be a strong predictor of ventricular arrhythmias with a 33-fold increase in odds for a significant arrhythmic event.[44] CMR has revealed hemorrhagic infarction and chronic iron deposition as potentially new physiological mechanisms of heart failure and arrhythmia in CAD.

Assessment of Extracellular Volume as a Novel Imaging Biomarker

The late gadolinium–enhanced technique has become an important imaging biomarker for the detection of focal fibrosis in both ischemic and nonischemic cardiomyopathies. However, several cardiac pathologies result in more diffuse alterations of the extracellular matrix, which are not easily detected using late gadolinium–enhanced. CMR T1 mapping techniques may be used in conjunction with magnetic resonance imaging contrast agents to quantify the expansion of the extracellular volume (ECV) resulting from inflammation, edema, infiltration, or fibrosis.

Measurement of ECV was first described in the late 1990s by Arheden et al,[45] who validated the technique using radioisotopes and light microscopy and demonstrated that ECV was 23% in normal myocardium and 90% in infarcted myocardium (Figure 4) The development of rapid breath-hold T1 cardiac mapping sequences, such as the MOLLI technique,[26] has

made ECV mapping clinically feasible. The relatively fast exchange kinetics of the contrast agent between the blood pool and myocardium, and slow excretion by the kidneys, enable stable measurement of ECV typically after 5 to 10 minutes after a bolus injection.[45–48] Thus, ECV measurement can easily be integrated into a standard clinical protocol.

The consensus statement on T1 mapping from the Society of Cardiovascular Magnetic Resonance, which is currently being updated, highlights several challenges and best practices for obtaining reliable assessment of T1 and ECV.[49] It is important to note that ECV expansion can be caused by several factors in addition to diffuse fibrosis, including edema, infiltration, or changes in intravascular volume. Thus, ECV can only be used as a surrogate maker for diffuse fibrosis when these other factors have been considered.

Clinical Validation and Utility

Clinical validation using biopsies to correlate collagen content to ECV was first performed after a bolus of GBCAs followed by an infusion using a regular late gadolinium–enhanced sequence[50] and later also using ECV mapping techniques after a single contrast injection.[51] The study by Ugander et al[48] nicely demonstrated the clinical utility of ECV mapping in patients with overt and subclinical myocardial pathology (Figure 5)

Several studies have demonstrated that T1 mapping and ECV mapping contribute mechanistic and prognostic insights into valve disease, infarction, and hypertension.[29,52] T1 and ECV have demonstrated potential utility in cases of suspected cardiomyopathy, infiltrative disease,[53] myocarditis,[30] and hypertrophic cardiomyopathy.[54] Widespread availability of fully automatic generation of ECV maps on the scanner will facilitate routine clinical use of this technique.[55]

Recent Developments in Non-Breath-Hold and Non-ECG-Gated CMR Techniques

Challenges of Conventional Techniques

Motion of the heart resulting from both cardiac and respiratory cycles remains a challenge for robust CMR imaging. In patients with shortness of breath, breath holding may be inadequate, resulting in image artifacts. Free-breathing CMR techniques which use navigators to track diaphragmatic motion have been implemented in most MR systems from all major vendors and have been used in many CMR applications, such as noncontrast whole-heart coronary MRA,[56] 3D myocardial T1 mapping,[57] and 3D cardiac diffusion-weighted CMR.[58] However, relatively low gating efficiency, typically between 30% and 50%, may result in lengthy and unpredictable imaging times, particularly with whole-heart imaging. Recent navigator techniques which retrospectively correct motion, such as Three-Dimensional Retrospective Image-Based Motion Correction (TRIM), can achieve nearly 100% gating efficiency.[59] Although clinically useful, diaphragmatic navigator gating provides an indirect measure of heart motion and requires time and expertise to set up correctly. Several factors can cause poor ECG gating, particularly at 3T, resulting in motion-induced artifacts. While real-time imaging can be performed without ECG triggering,

conventional techniques have reduced temporal or spatial resolution, limiting quality as compared with breath-held imaging.

Non-Breath-Hold and Non-ECG-Gated CMR Techniques

The CMR examination could be greatly simplified if high-quality images could be obtained without the need for breath holding or ECG gating, and this is an active area of CMR research. By significantly undersampling the raw data, it is possible to perform real-time CMR without ECG gating, which provides tolerance to arrhythmias. Non-Cartesian sampling patterns are often used for real-time cine imaging because they are more time-efficient and robust to flow and motion. With radial sampling and nonlinear inverse reconstruction with temporal regularization, Zhang et al[60] achieved a temporal resolution of 20 ms with online reconstruction using a graphical processing unit. Feng et al[61] showed improved signal-to-noise ratio, contrast-to-noise ratio, and image quality of spiral acquisition over radial sampling for real-time cine CMR. Sharif et al[5] used a continuous magnetization-driven radial sampling for non-ECG-gated myocardial perfusion magnetic resonance imaging. One of the problems with real-time CMR is limited temporal and spatial resolution. Kellman et al[62] developed a retrospective reconstruction method to improve temporal and spatial resolution of real-time cine by combining data acquired over multiple heartbeats using respiratory motion correction and rebinning of data.

Direct measurement of heart motion can be obtained from a self-navigator derived from the imaging data itself.[63] Image projections,[64] 2-dimensional images,[65] or 3D[66] images have been used to derive self-navigator signals. In more recent techniques, motion data for both respiratory gating and cardiac triggering can be extracted by filtering a self-gating projection because cardiac and respiratory motion have different temporal frequency ranges and information content (Figure 6). These methods have been used for 2-dimensional[67] and 3D cine imaging[68] and 4-dimensional whole-heart coronary MRA.[59] An alternative approach is to resolve cardiac and respiratory motion using a CS technique, such as XD-GRASP, as described earlier.[10] Although these techniques hold significant promise, they have yet to undergo significant clinical validation. These techniques may allow drastic simplification of the workflow or push-button CMR, which may facilitate the wide clinical application of CMR.

Other Emerging Clinical Techniques

There are several techniques on the verge of clinical translation which deserve mention but cannot be discussed in detail because of the scope of this review. Recent advances in diffusion-weighted CMR, such as diffusion tensor imaging, have enabled detailed assessment of myocardial fiber orientation. These techniques are providing novel physiological insights into cardiovascular physiology, such as the difference in sheet-let orientations in both dilated and hypertrophic cardiomyopathies.[69] Diffusion-weighted CMR imaging can detect edema and fibrosis in myocardial infarction. A recent study has demonstrated significant correlation between the apparent diffusion coefficient and ECV, suggesting that diffusion-weighted CMR imaging could be a noncontrast surrogate for ECV.[70] Current techniques are limited by long acquisition times, but advances in image

acquisition and reconstruction will make this technique clinically feasible. CMR has the ability to measure blood flow and noninvasively assess Qp/Qs, making it an indispensable tool in assessment of congenital heart disease. There has been growing interest in the technique of 4-dimensional flow imaging, which can simultaneously assess myocardial structure and function and blood flow dynamics within a single scan.[71] The technique holds promise for assessment of congenital heart disease and diseases of the aorta.[71] There has also been a growing interest in rapid assessment of myocardial strain, partially driven by the success of speckle tracking echocardiography. New techniques, such as displacement encoding with stimulated echoes (DENSE)[72] and feature tracking from cine imaging, are bringing CMR strain techniques into routine clinical practice.[73] Another area of active research is improving CMR imaging in the presence of cardiac devices. New techniques, such as wideband late gadolinium–enhanced, are extending the utility of CMR to the growing number of patients with implantable cardiac devices.[74]

Conclusions

The diagnostic and prognostic utility of CMR continues to evolve, with new techniques providing novel insights into cardiac pathophysiology and providing unprecedented tissue characterization of the myocardium. Novel acquisition strategies combined with advanced reconstruction techniques are enabling high-resolution, truly 3D dynamic acquisitions, which will be the future of CMR. Recent development of fast T1, T2, and T2* mapping techniques are rapidly entering the clinical CMR arsenal of techniques for tissue characterization. T1 mapping combined with GBCAs is enabling in vivo assessment of ECV, which is finding applications in multiple cardiac pathologies. Finally, limitations because of cardiac and respiratory motion are being overcome, which could revolutionize how CMR is performed in routine clinical practice and lead to more widespread clinical adoption of CMR.

References

1. Tsao J, Boesiger P, Pruessmann KP. k-t BLAST and k-t SENSE: dynamic MRI with high frame rate exploiting spatiotemporal correlations. Magn Reson Med. 2003; 50:1031–1042. DOI: 10.1002/mrm.10611 [PubMed: 14587014]
2. Pedersen H, Kozerke S, Ringgaard S, Nehrke K, Kim WY. k-t PCA: temporally constrained k-t BLAST reconstruction using principal component analysis. Magn Reson Med. 2009; 62:706–716. DOI: 10.1002/mrm.22052 [PubMed: 19585603]
3. Manka R, Jahnke C, Kozerke S, Vitanis V, Crelier G, Gebker R, Schnackenburg B, Boesiger P, Fleck E, Paetsch I. Dynamic 3-dimensional stress cardiac magnetic resonance perfusion imaging: detection of coronary artery disease and volumetry of myocardial hypoenhancement before and after coronary stenting. J Am Coll Cardiol. 2011; 57:437–444. DOI: 10.1016/j.jacc.2010.05.067 [PubMed: 21251584]
4. Otazo R, Kim D, Axel L, Sodickson DK. Combination of compressed sensing and parallel imaging for highly accelerated first-pass cardiac perfusion MRI. Magn Reson Med. 2010; 64:767–776. DOI: 10.1002/mrm.22463 [PubMed: 20535813]
5. Sharif B, Arsanjani R, Dharmakumar R, Bairey Merz CN, Berman DS, Li D. All-systolic non-ECG-gated myocardial perfusion MRI: Feasibility of multi-slice continuous first-pass imaging. Magn Reson Med. 2015; 74:1661–1674. DOI: 10.1002/mrm.25752 [PubMed: 26052843]

6. Yang Y, Kramer CM, Shaw PW, Meyer CH, Salerno M. First-pass myocardial perfusion imaging with whole-heart coverage using L1-SPIRiT accelerated variable density spiral trajectories. Magn Reson Med. 2016; 76:1375–1387. DOI: 10.1002/mrm.26014 [PubMed: 26538511]
7. Kim D, Dyvorne HA, Otazo R, Feng L, Sodickson DK, Lee VS. Accelerated phase-contrast cine MRI using k-t SPARSE-SENSE. Magn Reson Med. 2012; 67:1054–1064. DOI: 10.1002/mrm.23088 [PubMed: 22083998]
8. Mehta BB, Chen X, Bilchick KC, Salerno M, Epstein FH. Accelerated and navigator-gated look-locker imaging for cardiac T1 estimation (ANGIE): Development and application to T1 mapping of the right ventricle. Magn Reson Med. 2015; 73:150–160. DOI: 10.1002/mrm.25100 [PubMed: 24515952]
9. Feng L, Srichai MB, Lim RP, Harrison A, King W, Adluru G, Dibella EV, Sodickson DK, Otazo R, Kim D. Highly accelerated real-time cardiac cine MRI using k-t SPARSE-SENSE. Magn Reson Med. 2013; 70:64–74. DOI: 10.1002/mrm.24440 [PubMed: 22887290]
10. Feng L, Axel L, Chandarana H, Block KT, Sodickson DK, Otazo R. XD-GRASP: Golden-angle radial MRI with reconstruction of extra motion-state dimensions using compressed sensing. Magn Reson Med. 2016; 75:775–788. DOI: 10.1002/mrm.25665 [PubMed: 25809847]
11. Greenwood JP, Maredia N, Younger JF, Brown JM, Nixon J, Everett CC, Bijsterveld P, Ridgway JP, Radjenovic A, Dickinson CJ, Ball SG, Plein S. Cardiovascular magnetic resonance and single-photon emission computed tomography for diagnosis of coronary heart disease (CE-MARC): a prospective trial. Lancet. 2012; 379:453–460. DOI: 10.1016/S0140-6736(11)61335-4 [PubMed: 22196944]
12. Morton G, Chiribiri A, Ishida M, Hussain ST, Schuster A, Indermuehle A, Perera D, Knuuti J, Baker S, Hedström E, Schleyer P, O'Doherty M, Barrington S, Nagel E. Quantification of absolute myocardial perfusion in patients with coronary artery disease: comparison between cardiovascular magnetic resonance and positron emission tomography. J Am Coll Cardiol. 2012; 60:1546–1555. DOI: 10.1016/j.jacc.2012.05.052 [PubMed: 22999722]
13. Motwani M, Jogiya R, Kozerke S, Greenwood JP, Plein S. Advanced cardiovascular magnetic resonance myocardial perfusion imaging: high-spatial resolution versus 3-dimensional whole-heart coverage. Circ Cardiovasc Imaging. 2013; 6:339–348. DOI: 10.1161/CIRCIMAGING.112.000193 [PubMed: 23512780]
14. Manka R, Wissmann L, Gebker R, Jogiya R, Motwani M, Frick M, Reinartz S, Schnackenburg B, Niemann M, Gotschy A, Kuhl C, Nagel E, Fleck E, Marx N, Luescher TF, Plein S, Kozerke S. Multicenter evaluation of dynamic three-dimensional magnetic resonance myocardial perfusion imaging for the detection of coronary artery disease defined by fractional flow reserve. Circ Cardiovasc Imaging. 2015; 8:003061.doi: 10.1161/CIRCIMAGING.114.003061
15. Gerber BL, Raman SV, Nayak K, Epstein FH, Ferreira P, Axel L, Kraitchman DL. Myocardial first-pass perfusion cardiovascular magnetic resonance: history, theory, and current state of the art. J Cardiovasc Magn Reson. 2008; 10:18.doi: 10.1186/1532-429X-10-18 [PubMed: 18442372]
16. Manka R, Vitanis V, Boesiger P, Flammer AJ, Plein S, Kozerke S. Clinical feasibility of accelerated, high spatial resolution myocardial perfusion imaging. JACC Cardiovasc Imaging. 2010; 3:710–717. DOI: 10.1016/j.jcmg.2010.03.009 [PubMed: 20633848]
17. Salerno M, Sica C, Kramer CM, Meyer CH. Improved first-pass spiral myocardial perfusion imaging with variable density trajectories. Magn Reson Med. 2013; 70:1369–1379. DOI: 10.1002/mrm.24569 [PubMed: 23280884]
18. Salerno M, Sica CT, Kramer CM, Meyer CH. Optimization of spiral-based pulse sequences for first-pass myocardial perfusion imaging. Magn Reson Med. 2011; 65:1602–1610. DOI: 10.1002/mrm.22746 [PubMed: 21590802]
19. Salerno M, Taylor A, Yang Y, Kuruvilla S, Ragosta M, Meyer CH, Kramer CM. Adenosine stress cardiovascular magnetic resonance with variable-density spiral pulse sequences accurately detects coronary artery disease: initial clinical evaluation. Circ Cardiovasc Imaging. 2014; 7:639–646. DOI: 10.1161/CIRCIMAGING.113.001584 [PubMed: 24759900]
20. Sharif B, Dharmakumar R, LaBounty T, Arsanjani R, Shufelt C, Thomson L, Merz CN, Berman DS, Li D. Towards elimination of the dark-rim artifact in first-pass myocardial perfusion MRI: removing Gibbs ringing effects using optimized radial imaging. Magn Reson Med. 2014; 72:124–136. DOI: 10.1002/mrm.24913 [PubMed: 24030840]

21. Harrison A, Adluru G, Damal K, Shaaban AM, Wilson B, Kim D, McGann C, Marrouche NF, DiBella EV. Rapid ungated myocardial perfusion cardiovascular magnetic resonance: preliminary diagnostic accuracy. J Cardiovasc Magn Reson. 2013; 15:26.doi: 10.1186/1532-429X-15-26 [PubMed: 23537093]
22. Patel AR, Antkowiak PF, Nandalur KR, West AM, Salerno M, Arora V, Christopher J, Epstein FH, Kramer CM. Assessment of advanced coronary artery disease: advantages of quantitative cardiac magnetic resonance perfusion analysis. J Am Coll Cardiol. 2010; 56:561–569. DOI: 10.1016/j.jacc.2010.02.061 [PubMed: 20688211]
23. Mordini FE, Haddad T, Hsu LY, Kellman P, Lowrey TB, Aletras AH, Bandettini WP, Arai AE. Diagnostic accuracy of stress perfusion CMR in comparison with quantitative coronary angiography: fully quantitative, semiquantitative, and qualitative assessment. JACC Cardiovasc Imaging. 2014; 7:14–22. DOI: 10.1016/j.jcmg.2013.08.014 [PubMed: 24433707]
24. Thomson LE, Wei J, Agarwal M, Haft-Baradaran A, Shufelt C, Mehta PK, Gill EB, Johnson BD, Kenkre T, Handberg EM, Li D, Sharif B, Berman DS, Petersen JW, Pepine CJ, Bairey Merz CN. Cardiac magnetic resonance myocardial perfusion reserve index is reduced in women with coronary microvascular dysfunction. A National Heart, Lung, and Blood Institute-sponsored study from the Women's Ischemia Syndrome Evaluation. Circ Cardiovasc Imaging. 2015; 8:e002481.doi: 10.1161/CIRCIMAGING.114.002481 [PubMed: 25801710]
25. Salerno M, Kramer CM. Advances in parametric mapping with CMR imaging. JACC Cardiovasc Imaging. 2013; 6:806–822. DOI: 10.1016/j.jcmg.2013.05.005 [PubMed: 23845576]
26. Messroghli DR, Radjenovic A, Kozerke S, Higgins DM, Sivananthan MU, Ridgway JP. Modified Look-Locker inversion recovery (MOLLI) for high-resolution T1 mapping of the heart. Magn Reson Med. 2004; 52:141–146. DOI: 10.1002/mrm.20110 [PubMed: 15236377]
27. Piechnik SK, Ferreira VM, Dall'Armellina E, Cochlin LE, Greiser A, Neubauer S, Robson MD. Shortened Modified Look-Locker Inversion recovery (ShMOLLI) for clinical myocardial T1-mapping at 1.5 and 3 T within a 9 heartbeat breathhold. J Cardiovasc Magn Reson. 2010; 12:69.doi: 10.1186/1532-429X-12-69 [PubMed: 21092095]
28. Chow K, Flewitt JA, Green JD, Pagano JJ, Friedrich MG, Thompson RB. Saturation recovery single-shot acquisition (SASHA) for myocardial T(1) mapping. Magn Reson Med. 2014; 71:2082–2095. DOI: 10.1002/mrm.24878 [PubMed: 23881866]
29. Taylor AJ, Salerno M, Dharmakumar R, Jerosch-Herold M. T1 mapping: basic techniques and clinical applications. JACC Cardiovasc Imaging. 2016; 9:67–81. DOI: 10.1016/j.jcmg.2015.11.005 [PubMed: 26762877]
30. Luetkens JA, Homsi R, Sprinkart AM, Doerner J, Dabir D, Kuetting DL, Block W, Andrié R, Stehning C, Fimmers R, Gieseke J, Thomas DK, Schild HH, Naehle CP. Incremental value of quantitative CMR including parametric mapping for the diagnosis of acute myocarditis. Eur Heart J Cardiovasc Imaging. 2016; 17:154–161. DOI: 10.1093/ehjci/jev246 [PubMed: 26476398]
31. Bull S, White SK, Piechnik SK, Flett AS, Ferreira VM, Loudon M, Francis JM, Karamitsos TD, Prendergast BD, Robson MD, Neubauer S, Moon JC, Myerson SG. Human non-contrast T1 values and correlation with histology in diffuse fibrosis. Heart. 2013; 99:932–937. DOI: 10.1136/heartjnl-2012-303052 [PubMed: 23349348]
32. Ferreira VM, Piechnik SK, Dall'Armellina E, Karamitsos TD, Francis JM, Choudhury RP, Friedrich MG, Robson MD, Neubauer S. Non-contrast T1-mapping detects acute myocardial edema with high diagnostic accuracy: a comparison to T2-weighted cardiovascular magnetic resonance. J Cardiovasc Magn Reson. 2012; 14:42.doi: 10.1186/1532-429X-14-42 [PubMed: 22720998]
33. Karamitsos TD, Piechnik SK, Banypersad SM, Fontana M, Ntusi NB, Ferreira VM, Whelan CJ, Myerson SG, Robson MD, Hawkins PN, Neubauer S, Moon JC. Noncontrast T1 mapping for the diagnosis of cardiac amyloidosis. JACC Cardiovasc Imaging. 2013; 6:488–497. DOI: 10.1016/j.jcmg.2012.11.013 [PubMed: 23498672]
34. Ugander M, Bagi PS, Oki AJ, Chen B, Hsu LY, Aletras AH, Shah S, Greiser A, Kellman P, Arai AE. Myocardial edema as detected by pre-contrast T1 and T2 CMR delineates area at risk associated with acute myocardial infarction. JACC Cardiovasc Imaging. 2012; 5:596–603. DOI: 10.1016/j.jcmg.2012.01.016 [PubMed: 22698528]

35. Feng Y, He T, Carpenter JP, Jabbour A, Alam MH, Gatehouse PD, Greiser A, Messroghli D, Firmin DN, Pennell DJ. *In vivo* comparison of myocardial T1 with T2 and T2* in thalassaemia major. J Magn Reson Imaging. 2013; 38:588–593. DOI: 10.1002/jmri.24010 [PubMed: 23371802]
36. Sado DM, White SK, Piechnik SK, Banypersad SM, Treibel T, Captur G, Fontana M, Maestrini V, Flett AS, Robson MD, Lachmann RH, Murphy E, Mehta A, Hughes D, Neubauer S, Elliott PM, Moon JC. Identification and assessment of Anderson-Fabry disease by cardiovascular magnetic resonance noncontrast myocardial T1 mapping. Circ Cardiovasc Imaging. 2013; 6:392–398. DOI: 10.1161/CIRCIMAGING.112.000070 [PubMed: 23564562]
37. Liu A, Wijesurendra RS, Francis JM, Robson MD, Neubauer S, Piechnik SK, Ferreira VM. Adenosine stress and rest T1 mapping can differentiate between ischemic, infarcted, remote, and normal myocardium without the need for gadolinium contrast agents. JACC Cardiovasc Imaging. 2016; 9:27–36. DOI: 10.1016/j.jcmg.2015.08.018 [PubMed: 26684978]
38. Giri S, Chung YC, Merchant A, Mihai G, Rajagopalan S, Raman SV, Simonetti OP. T2 quantification for improved detection of myocardial edema. J Cardiovasc Magn Reson. 2009; 11:56.doi: 10.1186/1532-429X-11-56 [PubMed: 20042111]
39. Thavendiranathan P, Walls M, Giri S, Verhaert D, Rajagopalan S, Moore S, Simonetti OP, Raman SV. Improved detection of myocardial involvement in acute inflammatory cardiomyopathies using T2 mapping. Circ Cardiovasc Imaging. 2012; 5:102–110. DOI: 10.1161/CIRCIMAGING.111.967836 [PubMed: 22038988]
40. Verhaert D, Thavendiranathan P, Giri S, Mihai G, Rajagopalan S, Simonetti OP, Raman SV. Direct T2 quantification of myocardial edema in acute ischemic injury. JACC Cardiovasc Imaging. 2011; 4:269–278. DOI: 10.1016/j.jcmg.2010.09.023 [PubMed: 21414575]
41. Tanner MA, Galanello R, Dessi C, Smith GC, Westwood MA, Agus A, Roughton M, Assomull R, Nair SV, Walker JM, Pennell DJ. A randomized, placebo-controlled, double-blind trial of the effect of combined therapy with deferoxamine and deferiprone on myocardial iron in thalassemia major using cardiovascular magnetic resonance. Circulation. 2007; 115:1876–1884. DOI: 10.1161/CIRCULATIONAHA.106.648790 [PubMed: 17372174]
42. Reffelmann T, Kloner RA. Microvascular reperfusion injury: rapid expansion of anatomic no reflow during reperfusion in the rabbit. Am J Physiol Heart Circ Physiol. 2002; 283:H1099–H1107. DOI: 10.1152/ajpheart.00270.2002 [PubMed: 12181140]
43. Kali A, Kumar A, Cokic I, Tang RL, Tsaftaris SA, Friedrich MG, Dharmakumar R. Chronic manifestation of postreperfusion intramyocardial hemorrhage as regional iron deposition: a cardiovascular magnetic resonance study with ex vivo validation. Circ Cardiovasc Imaging. 2013; 6:218–228. DOI: 10.1161/CIRCIMAGING.112.000133 [PubMed: 23403335]
44. Cokic I, Kali A, Yang HJ, Yee R, Tang R, Tighiouart M, Wang X, Jackman WS, Chugh SS, White JA, Dharmakumar R. iron-sensitive cardiac magnetic resonance imaging for prediction of ventricular arrhythmia risk in patients with chronic myocardial infarction: early evidence. Circ Cardiovasc Imaging. 2015; 8:e003642.doi: 10.1161/CIRCIMAGING.115.003642 [PubMed: 26259581]
45. Arheden H, Saeed M, Higgins CB, Gao DW, Bremerich J, Wyttenbach R, Dae MW, Wendland MF. Measurement of the distribution volume of gadopentetate dimeglumine at echoplanar MR imaging to quantify myocardial infarction: comparison with 99mTc-DTPA autoradiography in rats. Radiology. 1999; 211:698–708. DOI: 10.1148/radiology.211.3.r99jn41698 [PubMed: 10352594]
46. Wendland MF, Saeed M, Lauerma K, Derugin N, Mintorovitch J, Cavagna FM, Higgins CB. Alterations in T1 of normal and reperfused infarcted myocardium after Gd-BOPTA versus GD-DTPA on inversion recovery EPI. Magn Reson Med. 1997; 37:448–456. [PubMed: 9055236]
47. Arheden H, Saeed M, Higgins CB, Gao DW, Ursell PC, Bremerich J, Wyttenbach R, Dae MW, Wendland MF. Reperfused rat myocardium subjected to various durations of ischemia: estimation of the distribution volume of contrast material with echoplanar MR imaging. Radiology. 2000; 215:520–528. DOI: 10.1148/radiology.215.2.r00ma38520 [PubMed: 10796935]
48. Ugander M, Oki AJ, Hsu LY, Kellman P, Greiser A, Aletras AH, Sibley CT, Chen MY, Bandettini WP, Arai AE. Extracellular volume imaging by magnetic resonance imaging provides insights into overt and sub-clinical myocardial pathology. Eur Heart J. 2012; 33:1268–1278. DOI: 10.1093/eurheartj/ehr481 [PubMed: 22279111]

49. Moon JC, Messroghli DR, Kellman P, Piechnik SK, Robson MD, Ugander M, Gatehouse PD, Arai AE, Friedrich MG, Neubauer S, Schulz-Menger J, Schelbert EB. Society for Cardiovascular Magnetic Resonance Imaging; Cardiovascular Magnetic Resonance Working Group of the European Society of Cardiology. Myocardial T1 mapping and extracellular volume quantification: a Society for Cardiovascular Magnetic Resonance (SCMR) and CMR Working Group of the European Society of Cardiology consensus statement. J Cardiovasc Magn Reson. 2013; 15:92.doi: 10.1186/1532-429X-15-92 [PubMed: 24124732]
50. Flett AS, Hayward MP, Ashworth MT, Hansen MS, Taylor AM, Elliott PM, McGregor C, Moon JC. Equilibrium contrast cardiovascular magnetic resonance for the measurement of diffuse myocardial fibrosis: preliminary validation in humans. Circulation. 2010; 122:138–144. DOI: 10.1161/CIRCULATIONAHA.109.930636 [PubMed: 20585010]
51. Fontana M, White SK, Banypersad SM, Sado DM, Maestrini V, Flett AS, Piechnik SK, Neubauer S, Roberts N, Moon JC. Comparison of T1 mapping techniques for ECV quantification. Histological validation and reproducibility of ShMOLLI versus multibreath-hold T1 quantification equilibrium contrast CMR. J Cardiovasc Magn Reson. 2012; 14:88.doi: 10.1186/1532-429X-14-88 [PubMed: 23272651]
52. Kuruvilla S, Janardhanan R, Antkowiak P, Keeley EC, Adenaw N, Brooks J, Epstein FH, Kramer CM, Salerno M. Increased extracellular volume and altered mechanics are associated with LVH in hypertensive heart disease, not hypertension alone. JACC Cardiovasc Imaging. 2015; 8:172–180. DOI: 10.1016/j.jcmg.2014.09.020 [PubMed: 25577446]
53. Mongeon FP, Jerosch-Herold M, Coelho-Filho OR, Blankstein R, Falk RH, Kwong RY. Quantification of extracellular matrix expansion by CMR in infiltrative heart disease. JACC Cardiovasc Imaging. 2012; 5:897–907. DOI: 10.1016/j.jcmg.2012.04.006 [PubMed: 22974802]
54. Ho CY, Abbasi SA, Neilan TG, Shah RV, Chen Y, Heydari B, Cirino AL, Lakdawala NK, Orav EJ, González A, López B, Díez J, Jerosch-Herold M, Kwong RY. T1 measurements identify extracellular volume expansion in hypertrophic cardiomyopathy sarcomere mutation carriers with and without left ventricular hypertrophy. Circ Cardiovasc Imaging. 2013; 6:415–422. DOI: 10.1161/CIRCIMAGING.112.000333 [PubMed: 23549607]
55. Kellman P, Wilson JR, Xue H, Ugander M, Arai AE. Extracellular volume fraction mapping in the myocardium, part 1: evaluation of an automated method. J Cardiovasc Magn Reson. 2012; 14:63.doi: 10.1186/1532-429X-14-63 [PubMed: 22963517]
56. Stuber M, Botnar RM, Danias PG, Kissinger KV, Manning WJ. Submillimeter three-dimensional coronary MR angiography with real-time navigator correction: comparison of navigator locations. Radiology. 1999; 212:579–587. DOI: 10.1148/radiology.212.2.r99au50579 [PubMed: 10429721]
57. Weingärtner S, Akçakaya M, Roujol S, Basha T, Stehning C, Kissinger KV, Goddu B, Berg S, Manning WJ, Nezafat R. Free-breathing post-contrast three-dimensional T1 mapping: Volumetric assessment of myocardial T1 values. Magn Reson Med. 2015; 73:214–222. DOI: 10.1002/mrm.25124 [PubMed: 24554395]
58. Nguyen C, Fan Z, Sharif B, He Y, Dharmakumar R, Berman DS, Li D. *In vivo* three-dimensional high resolution cardiac diffusion-weighted MRI: a motion compensated diffusion-prepared balanced steady-state free precession approach. Magn Reson Med. 2014; 72:1257–1267. DOI: 10.1002/mrm.25038 [PubMed: 24259113]
59. Pang J, Bhat H, Sharif B, Fan Z, Thomson LE, LaBounty T, Friedman JD, Min J, Berman DS, Li D. Whole-heart coronary MRA with 100% respiratory gating efficiency: self-navigated three-dimensional retrospective image-based motion correction (TRIM). Magn Reson Med. 2014; 71:67–74. DOI: 10.1002/mrm.24628 [PubMed: 23401157]
60. Zhang S, Uecker M, Voit D, Merboldt KD, Frahm J. Real-time cardiovascular magnetic resonance at high temporal resolution: radial FLASH with nonlinear inverse reconstruction. J Cardiovasc Magn Reson. 2010; 12:39.doi: 10.1186/1532-429X-12-39 [PubMed: 20615228]
61. Feng X, Salerno M, Kramer CM, Meyer CH. Non-Cartesian balanced steady-state free precession pulse sequences for real-time cardiac MRI. Magn Reson Med. 2016; 75:1546–1555. DOI: 10.1002/mrm.25738 [PubMed: 25960254]
62. Kellman P, Chefd'hotel C, Lorenz CH, Mancini C, Arai AE, McVeigh ER. High spatial and temporal resolution cardiac cine MRI from retrospective reconstruction of data acquired in real

time using motion correction and resorting. Magn Reson Med. 2009; 62:1557–1564. DOI: 10.1002/mrm.22153 [PubMed: 19780155]

63. Larson AC, White RD, Laub G, McVeigh ER, Li D, Simonetti OP. Self-gated cardiac cine MRI. Magn Reson Med. 2004; 51:93–102. DOI: 10.1002/mrm.10664 [PubMed: 14705049]
64. Lai P, Larson AC, Park J, Carr JC, Li D. Respiratory self-gated four-dimensional coronary MR angiography: a feasibility study. Magn Reson Med. 2008; 59:1378–1385. DOI: 10.1002/mrm.21617 [PubMed: 18506786]
65. Aitken AP, Henningsson M, Botnar RM, Schaeffter T, Prieto C. 100% Efficient three-dimensional coronary MR angiography with two-dimensional beat-to-beat translational and bin-to-bin affine motion correction. Magn Reson Med. 2015; 74:756–764. DOI: 10.1002/mrm.25460 [PubMed: 25236813]
66. Addy NO, Ingle RR, Luo J, Baron CA, Yang PC, Hu BS, Nishimura DG. 3D image-based navigators for coronary MR angiography. Magn Reson Med. 2017; 77:1874–1883. DOI: 10.1002/mrm.26269 [PubMed: 27174590]
67. Buehrer M, Curcic J, Boesiger P, Kozerke S. Prospective self-gating for simultaneous compensation of cardiac and respiratory motion. Magn Reson Med. 2008; 60:683–690. DOI: 10.1002/mrm.21697 [PubMed: 18727084]
68. Liu J, Spincemaille P, Codella NC, Nguyen TD, Prince MR, Wang Y. Respiratory and cardiac self-gated free-breathing cardiac CINE imaging with multiecho 3D hybrid radial SSFP acquisition. Magn Reson Med. 2010; 63:1230–1237. DOI: 10.1002/mrm.22306 [PubMed: 20432294]
69. Nielles-Vallespin S, Khalique Z, Ferreira PF, de Silva R, Scott AD, Kilner P, McGill LA, Giannakidis A, Gatehouse PD, Ennis D, Aliotta E, Al-Khalil M, Kellman P, Mazilu D, Balaban RS, Firmin DN, Arai AE, Pennell DJ. Assessment of myocardial microstructural dynamics by *in vivo* diffusion tensor cardiac magnetic resonance. J Am Coll Cardiol. 2017; 69:661–676. DOI: 10.1016/j.jacc.2016.11.051 [PubMed: 28183509]
70. Nguyen C, Lu M, Fan Z, Bi X, Kellman P, Zhao S, Li D. Contrast-free detection of myocardial fibrosis in hypertrophic cardiomyopathy patients with diffusion-weighted cardiovascular magnetic resonance. J Cardiovasc Magn Reson. 2015; 17:107.doi: 10.1186/s12968-015-0214-1 [PubMed: 26631061]
71. Dyverfeldt P, Bissell M, Barker AJ, Bolger AF, Carlhäll CJ, Ebbers T, Francios CJ, Frydrychowicz A, Geiger J, Giese D, Hope MD, Kilner PJ, Kozerke S, Myerson S, Neubauer S, Wieben O, Markl M. 4D flow cardiovascular magnetic resonance consensus statement. J Cardiovasc Magn Reson. 2015; 17:72.doi: 10.1186/s12968-015-0174-5 [PubMed: 26257141]
72. Zhong X, Spottiswoode BS, Meyer CH, Kramer CM, Epstein FH. Imaging three-dimensional myocardial mechanics using navigator-gated volumetric spiral cine DENSE MRI. Magn Reson Med. 2010; 64:1089–1097. DOI: 10.1002/mrm.22503 [PubMed: 20574967]
73. Pedrizzetti G, Claus P, Kilner PJ, Nagel E. Principles of cardiovascular magnetic resonance feature tracking and echocardiographic speckle tracking for informed clinical use. J Cardiovasc Magn Reson. 2016; 18:51.doi: 10.1186/s12968-016-0269-7 [PubMed: 27561421]
74. Rashid S, Rapacchi S, Vaseghi M, Tung R, Shivkumar K, Finn JP, Hu P. Improved late gadolinium enhancement MR imaging for patients with implanted cardiac devices. Radiology. 2014; 270:269–274. DOI: 10.1148/radiol.13130942 [PubMed: 24086074]

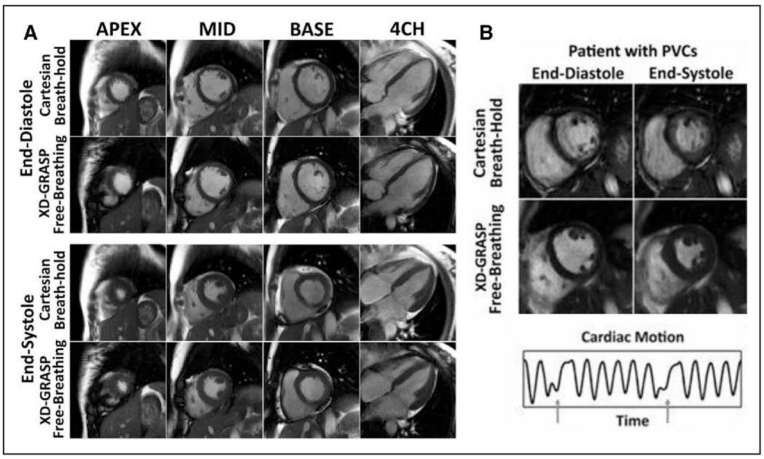

Figure 1.

Free-breathing Extra-Dimensional Golden-angle Radial Sparse Parallel Imaging (XD-GRASP) cine imaging. **A**, In a patient without arrhythmia, free-breathing XD-GRASP has similar image quality to standard breath-held acquisition. **B**, In a patient with premature ventricular contractions, XD-GRASP produces high-quality cine images, while reference breath-held technique demonstrates ghosting artifacts. Images are reconstructed as 2-dimensional (2D) arrays of physiological phases, permitting study of cardiorespiratory interactions. Reproduced from Feng et al[10] with permission of the publisher. Copyright ©2015, John Wiley and Sons.

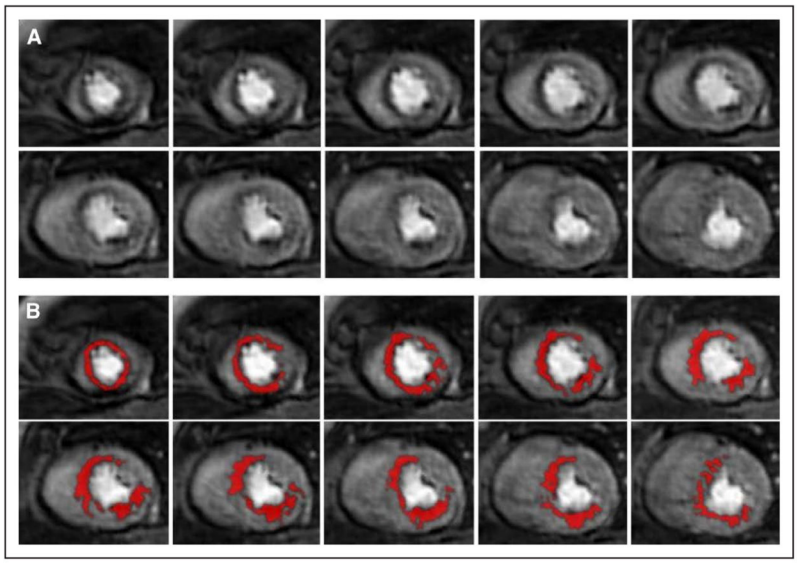

Figure 2.

Enabling quantification of myocardial ischemic burden using 3-dimensional (3D) whole-heart perfusion cardiovascular magnetic resonance imaging (CMR). **A**, Consecutive slices of a 3D perfusion CMR scan during adenosine stress in a patient with 3-vessel coronary artery disease (CAD). The acquired voxel size is 2.3×2.3×10 mm^3. **B**, Identical images illustrating volumetry of perfusion defects using a signal intensity threshold of 2 SD below the remote myocardium for the hypoenhanced regions (**red areas**). The ischemic burden (volume of myocardial hypoenhancement) was 24% of the total myocardium. Reprinted from *Journal of the American College of Cardiology*, 57.4, Manka et al, Dynamic 3-Dimensional Stress Cardiac Magnetic Resonance Perfusion Imaging Detection of Coronary Artery Disease and Volumetry of Myocardial Hypoenhancement Before and After Coronary Stenting, pages 437–444, Copyright 2011, with permission of American College of Cardiology Foundation.

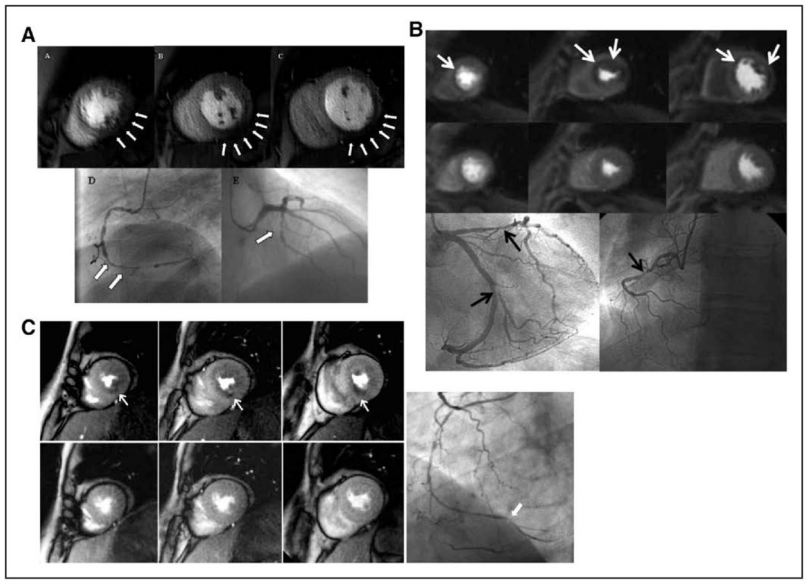

Figure 3.

Enabling improved subendocardial perfusion imaging using high-resolution and non-Cartesian cardiovasular magnetic resonance imaging (CMR). **A**, High-resolution (1.4 mm in-plane) stress perfusion CMR with Cartesian sampling at 1.5T using 5-fold acceleration with k-t BLAST reconstruction demonstrates subendocardial stress-induced perfusion defects in the inferior and inferolateral walls. Angiography revealed a subtotal occlusion of the right coronary artery and a significant stenosis in the left circumflex coronary artery territory. Reprinted from Manka et al[16] with permission of the publisher. Copyright ©2010, Elsevier. **B**, Non-Cartesian adenosine perfusion CMR with spiral sampling at 1.5T at stress (**top**) and rest (**bottom**) demonstrates subendocardial perfusion abnormality in the anterior and lateral walls (arrows). Coronary angiogram demonstrated multivessel-coronary artery disease (CAD). Variable density spiral sampling with apodization can detect subendocardial defects without dark-rim artifacts. Reprinted from Salerno et al[19] with permission of the publisher. Copyright ©2014, Wolters Kluwer Health, Inc. **C**, High-resolution (1.4 mm) non-Cartesian perfusion CMR performed using non-ECG-gated continuous acquisition radial sampling enables systolic imaging of all slices at 3T at stress (**top**) and rest (**bottom**) in a patient with a history of CAD and prior revascularization. A transmural perfusion gradient with hypoperfused subendocardium in the inferior wall is consistent with the chronic total occlusion of the right coronary artery shown by angiography. Continuous radial acquisition achieves high-resolution systolic imaging without ECG-gating, which is free of dark-rim artifact. Reprinted from Sharif et al[5] with permission of the publisher. Copyright ©2015, John Wiley and Sons.

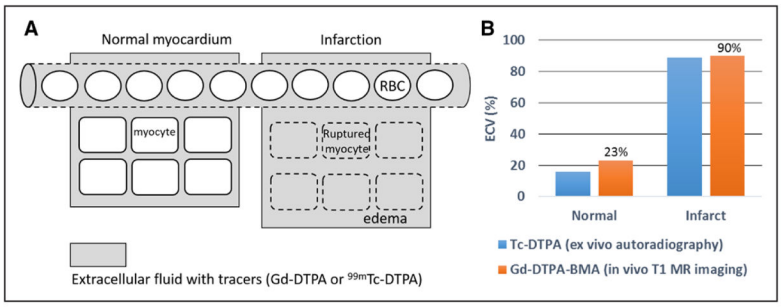

Figure 4.

A, Tissue distribution of extracellular tracers in normal and reperfused infarcted myocardium. **B**, Extracellular volume (ECV) measurements by magnetic resonance (MR) imaging in vivo in normal and infarcted rat myocardium after a single injection of Gd-DTPA-BMA (orange bars). T1 measurements were performed in ROIs on single-shot echo-planar inversion recovery MR images (TR 7000 ms). Blue bars show validation experiments by independent radioisotope autoradiography technique using 99mTc-DTPA ex vivo. The ECV in normal myocardium by MR imaging was 23±2% and the corresponding value in infarcted myocardium was 90±5%, indicating almost complete necrosis. Reproduced from Arheden et al[45] with permission of the publisher. Copyright ©1999, Radiological Society of North America.

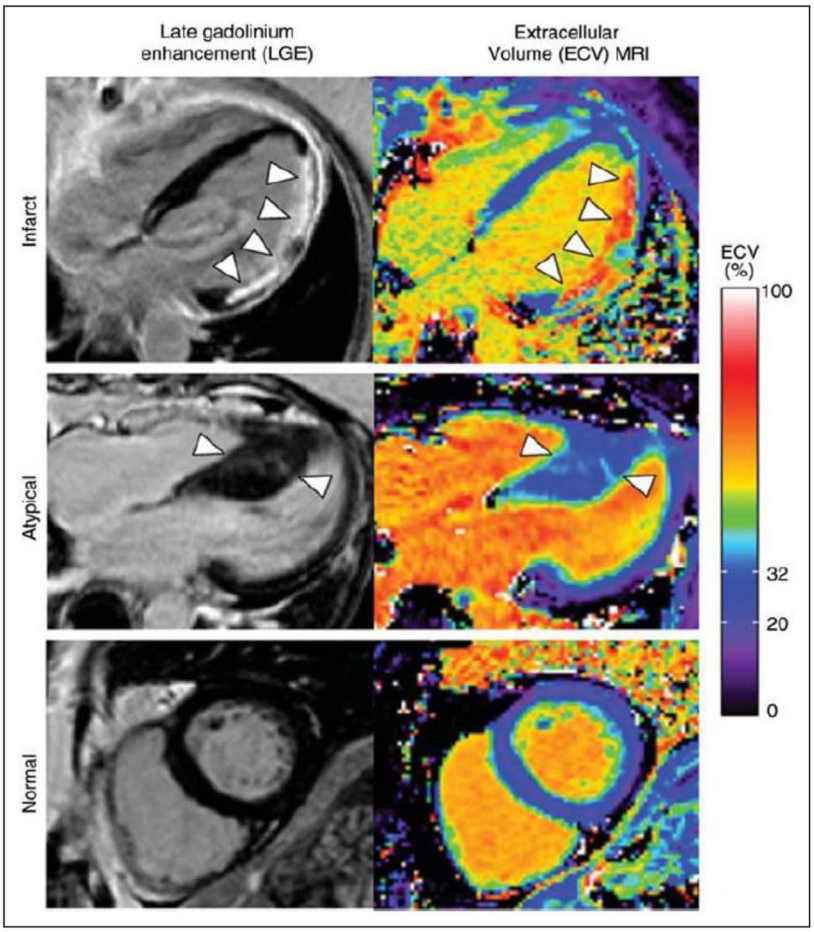

Figure 5.

Three examples of late gadolinium–enhanced (LGE) images (**left column**) and corresponding extracellular volume (ECV) maps (**right column**) in patients with lateral infarction (**top row**), hypertrophied cardiomyopathy (**middle row**), and normal myocardium (**bottom row**). All images acquired after a single magnetic resonance (MR) contrast injection. ECV maps can contribute information on subtle myocardial diseases. Reprinted from Ugander et al[48] with permission of the publisher. Copyright ©2012, Oxford University Press.

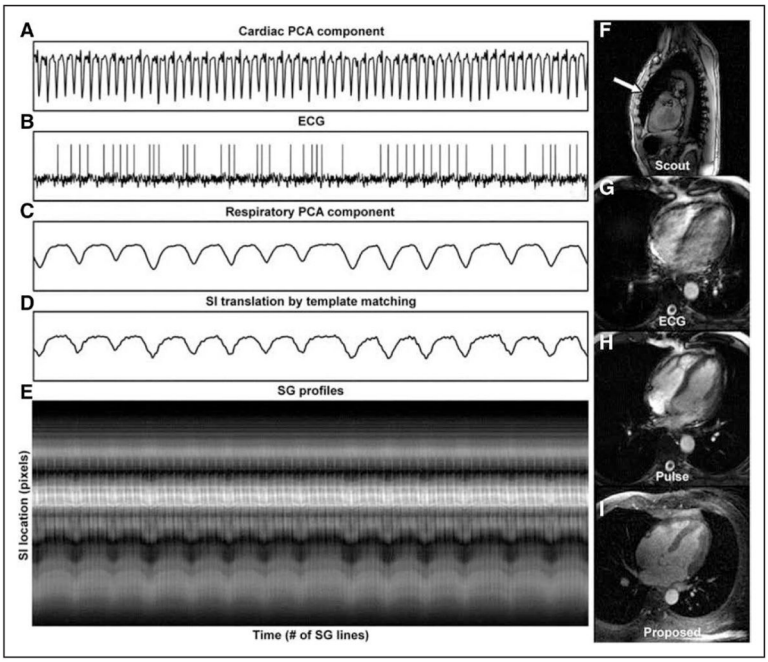

Figure 6.

A case of failed ECG triggering (**A**) cardiac component. **B**, ECG waveform. **C**, Respiratory component. **D**, Superior-inferior (SI) translation detected by template matching. **E**, Self gating (SG) projection time series. The cardiac SG waveform showed distinct valleys as triggering features. **F**, The ECG waveform yielded incorrect triggers, likely caused by the chest deformity shown in the sagittal scout image. **G**, The ECG-triggered cine image showed significant blurring because of the unresolved cardiac motion. **H**, Switching to pulse triggering improved the image quality. **I**, The same 4-chamber view was reformatted from the self-gated 4D series, showing excellent image quality. Reprinted from Pang et al[59] with permission of the publisher. Copyright ©2014, John Wiley and Sons.